DESIGN AND PERFORMANCE TEST OF REMOTE DRIVING CONTROL SYSTEM OF SMALL AGRICULTURAL HYDRAULIC CHASSIS
/
小型农用液压底盘远程驾驶控制系统的设计与试验

Xiaorong LÜ[#1)], Yuan FU[#1)], Xinping CHENG[2)], Fugui ZHANG[1)], Yuancai LEN[1)], Dandan HAN[1*)]
[1)] College of Machinery & Electronics, Sichuan Agricultural University, Yaan, Sichuan, 625014, China
[2)]Chengdu Wenjiang Science and Technology Industrial Development Park, Chengdu, Sichuan, 611130, China
[*]*Corresponding author's Email: handan1988@126.com*
DOI: https://doi.org/10.35633/inmateh-72-24

Keywords: *Agricultural chassis, Remote control, Mathematical model, System design, Test.*

ABSTRACT
Aiming at the adaptability and safety problems of agricultural machinery in hilly and mountainous areas, the remote driving control system of agricultural full hydraulic chassis is designed based on ARM-Linux platform. The whole remote driving system is composed of Web upper computer, server system and chassis drive system. According to the requirements of chassis operation, the STM32F407 is used as the lower computer to realize the running control and motion status monitoring of the chassis. Taking the I.MX6ULL as the hardware platform, the Linux as the software platform, and 4G communications as the Web Server, the remote driving of the chassis is realized through Web pages on the computer. It can be seen from the test results that the minimum RTT delay from the Web page driving to the lower computer is 170 ms; the maximum RTT delay is 1310 ms, and the average RTT delay is 222.75 ms. The real-time interactivity of the control system meets the needs of remote driving of the agricultural machinery. The research provides a theoretical basis and technical reference for the development of the remote driving system of the agricultural machinery.

摘要
针对丘陵山区农机具作业适应性、安全性存在的问题，基于 ARM-Linux 平台设计了农用全液压底盘的远程驾驶控制系统。整个远程驾驶系统由 Web 上位机、服务器系统和底盘驱动系统组成。根据底盘作业需求，以 STM32F407 为下位机，实现底盘的行走控制和运行状态监测；以 I.MX6ULL 为硬件平台、以 Linux 为软件平台、基于 4G 通信搭建 Web 服务器，实现在计算机上通过 Web 网页远程驾驶底盘。由测试结果可知，Web 网页驾驶端到下位机的最小 RTT 延时为 170ms，最大 RTT 延时为 1310ms，平均 RTT 延时为 222.75ms，控制系统的实时交互性满足远程驾驶农机具的需要，研究为农用底盘远程驾驶系统的开发提供了理论依据与技术参考。

INTRODUCTION
Due to complex ground conditions, small and micro agricultural machines are more suitable for hilly and mountainous areas *(Wang et al.,2022; Liu, 2018)*. But these agricultural machines have the problems such as poor operation adaptability and manned driving safety. These have resulted in low agricultural mechanization and high agricultural labor costs, restricting the agricultural economic developments in these areas *(Liu et al., 2020; Zheng et al., 2020; Wu et al., 2022)*. Autonomous driving can engage in agricultural production all day to solve these problems of agricultural machinery in hilly and mountainous areas *(Roshanianfard et al., 2020; Zhang et al., 2018; Yang et al., 2021)*. Remote driving can indirectly control the agricultural machinery through the network, improve driving safety, and reduce the demand for labor. Many researches on vehicle remote driving have been carried out to improve vehicle adaptability and controllability *(Alinaghi Hosseinabadi et al., 2020; Zhou et al., 2019; Geetha et al., 2020; Wang et al., 2020; Kim, 2019; Aliff et al., 2019; Cuenca et al., 2019; Han et al., 2022)*. Taking the radio technology as a communication means and a hand-held remote controller as a remote control terminal, *Gázquez et al. (2016)* designed and implemented a remote driving system for agricultural machinery. *Chu et al. (2018)* developed a WIFI based-remote driving intelligent agricultural mobile robot. *Wang et al. (2018)* designed a remote control system for tracked vehicles based on LAN and machine vision. The control system cannot transmit images and has short controllable distance.

Xiaorong LÜ, Professor; Yuan FU, M.S. Student; Xinping CHENG, Engineer; Fugui ZHANG, M.S. Student; Yuancai LEN, M.S. Student; Dandan HAN, Associate Professor.
(#Theses authors contributed to the work equally and should be regarded as co-first authors.)

Heikkilä et al. (2021) designed a remote driving control system on a driving Simulator, which increased the cost and reduced the portability of operation. Based on the Web page and the 4G network, the remote driving control system of agricultural full hydraulic chassis is developed. The study provides a theoretical and technical basis for the development of agricultural machines in hilly and mountainous areas.

MATERIALS AND METHODS

Design of The Hydraulic Drive System

The structure of the chassis hydraulic drive system is shown in Figure 1.

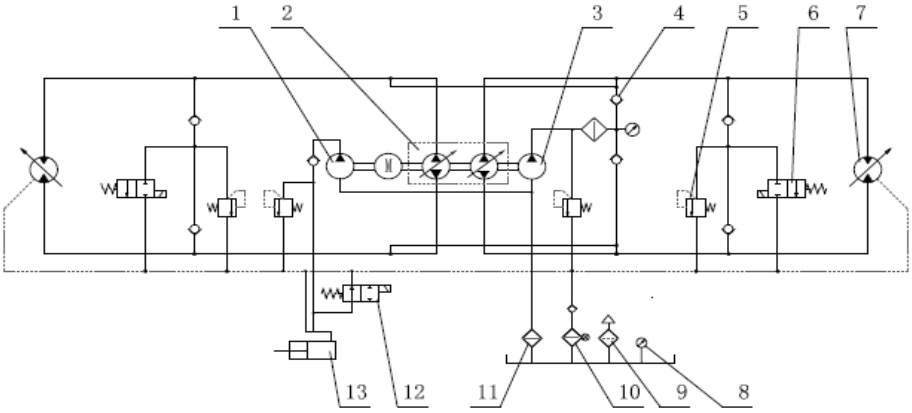

Fig. 1 - Hydraulic drive system diagram of the chassis

1, 3.- Gear pump; 2 - Double-pump; 4 - One-way valve; 5 - Overflow valve; 6, 12 - Electromagnetism reversing valve; 7 - Hydraulic motor; 8 - Pressure gauge; 9 - Air filter; 10, 11 - Oil filter; 13 – Cylinder

When the engine rotates, the transfer case outputs the power to drive the double-pump and gear pump. The power output of the hydraulic system is divided into two routes. When the handle of the double-pump rotates, the valve of the double-pump opens to control the flow of hydraulic oil. Then the hydraulic oil enters the hydraulic motor through the double-pump, and the output shafts of the motor drives the wheels on the chassis to achieve walking. When the handle of the hydraulic control valve is pressed, the gear pump opens and the hydraulic oil enters the hydraulic cylinder through the hydraulic control valve. The hydraulic control valve controls the motion parameters of the cylinder through its flow rate, driving the movement of small agricultural machinery behind the chassis.

Establishment of Control Mathematical Model

The controlled object is a hydraulic chassis powered by a diesel engine. The valve handle of the double-pump is connected to the output shaft of the electric steering gear. Through changing the angle of the steering gear, the opening of the double-pump valve can be changed to control the output speed of the motor. The motor changes the track speed and motion state of the chassis through the drive wheels. The control process of the chassis is shown in Figure 2.

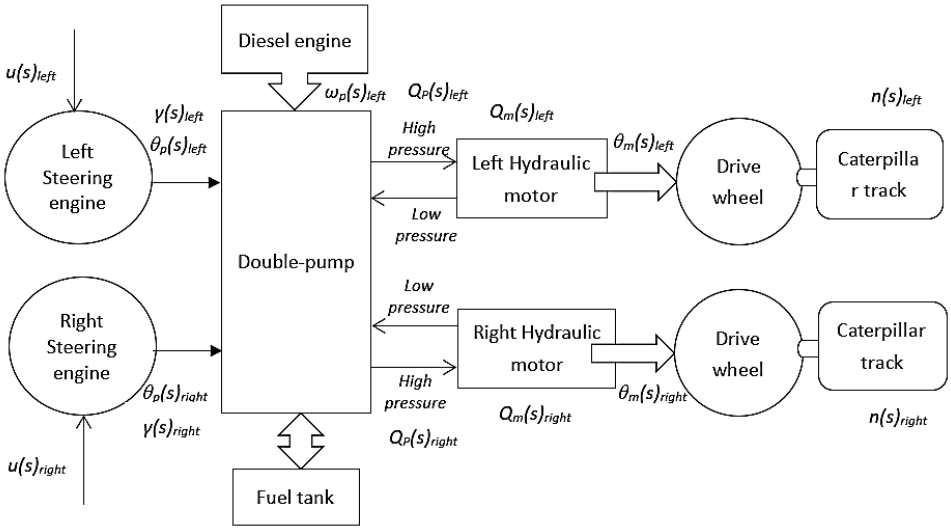

Fig. 2 - Structure of the chassis control

The driving system controls the output speed of the hydraulic motor through an electric steering gear to control the output displacement of the dual pump, realizing the stepless speed regulation of the chassis. Under the action of the controller, the steering gear outputs the angle through the DC motor and the reduction gear. The relationship between the parameters in the dynamic process is analyzed, and the mathematical model of system control is established. The voltage balance of the DC motor is calculated as follows:

$$u(t) = Li'(t) + Ri(t) + K_e\theta_m'(t) \tag{1}$$

where u is the DC motor circuit voltage, V; L is the DC motor inductance, H; R is the DC motor resistance, Ω; I is the DC motor current, A; K_e is the back EMF Constant, V.s/rad, and θ_m is the output angle of DC motor, rad.

The relationship between the DC motor current and output torque is as follows:

$$T = K_T i \tag{2}$$

where T is the DC motor torque, N. m, and K_T is the torque coefficient of DC motor, N· m/A.

The torque balance of the DC motor is calculated as follows:

$$T(t) = J\theta_m''(t) + B_v\theta_m'(t) + M_L \tag{3}$$

where J is the moment of inertia, kg·m^2; B_v is the DC motor damping coefficient, N·s/m; M_L is the equivalent load torque on output shaft of DC motor, N·m.

Through the Laplace transformation of Eqs. (1), (2) and (3), the transfer function of voltage and output angle of the DC motor is as follows:

$$\frac{\theta_m(s)}{u(s)} = \frac{1}{K_e\left(T_m s^2 + s\right)} \tag{4}$$

where T_e is the electrical time constant, s.

The transfer function of the motor output angle and steering gear angle is:

$$\theta_p(s) = K_i\theta_m(s) \tag{5}$$

where K_i -transmission ratio of reduction gear set.

Combined with Eqs.(4) and (5), the transfer function of the DC motor input voltage and the steering gear output angle is as follows:

$$\frac{\theta_p(s)}{u(s)} = \frac{K_i}{K_e\left(T_m s^2 + s\right)} \tag{6}$$

To simplify the modeling process, it is assumed to model under ideal conditions. Setting the speed ω_p of the engine to the variable displacement pump is constant, and ignoring the oil pressure $p_r$of low pressure side, the flow continuity of the hydraulic pump is as follows:

$$Q_p(s) = k_p\omega_p\gamma(s) - C_{tp}p_l(s) \tag{7}$$

where Q_p is the output flow of variable displacement pump, m^3/s; k_p is the displacement gradient of variable displacement pump, m^3/rad^2; γ is the swashplate swing angle of variable displacement pump, rad; ω_p is the operating speed of variable displacement pump, rad/s; p_l is the oil pressure of high-pressure side, Pa; C_{tp} is the total leakage coefficient of the variable displacement pump.

Similarly, ignoring the oil pressure of the low-pressure side, the flow of the high-pressure side of the hydraulic motor is:

$$Q_p(s) = C_{tm}p_l(s) + D_m(s)\theta(s)s + \frac{V_0}{\beta_e}p_l(s)s \tag{8}$$

where C_{tm} is the total leakage coefficient of hydraulic motor, m^5/(N·s); D_m is the hydraulic motor displacement, m^3/rad; V_0 is the total volume of pump control system working chamber and loop connecting pipe, m^3; θ is the output angle of the hydraulic motor, rad.

The torque dynamics of the hydraulic motor and load is as follows:

$$D_m(s)p_l(s) = J_t\theta(s)s^2 + B_m\theta(s)s + G\theta(s) + T_L \tag{9}$$

where J_t - total moment of inertia of hydraulic motor and load, N·m·s^2; B_m -total viscous damping coefficient of hydraulic motor and load, N·m·s/rad; G - Stiffness of load, N·m/rad; T_L - Load torque, N·m.

Assuming the system is a rigid load (G=0) and combined with Eqs. (7), (8) and (9), the transfer function between the swashplate swing angle γ of the variable displacement pump and the output angle θ of the hydraulic motor is as follows:

$$\frac{\theta(s)}{\gamma(s)} = \frac{k_p w_p \omega_h^2}{D_m\left(s^2 + 2\omega_h \xi s + \omega_h^2\right)} \tag{10}$$

where ω_h is the natural frequency of the motor, and ξ is the damping ratio.

The relationship between the two is simplified linearly, as follows:

$$\gamma(s) = K_p \theta_p(s) \tag{11}$$

In actual operation, there will be a certain delay when the output shaft of the steering gear reaches the required angle. There will also be a certain delay when the controlled hydraulic motor pressure by the hydraulic pump reaches the required pressure. Therefore, considering the time-delay link of the system and combined with Eqs. (6), (10) and (11), the transfer function between the input voltage u of the steering gear and the output angle θ of the hydraulic motor is as follows:

$$\frac{\theta(s)}{u(s)} = \frac{K_p k_p \omega_p \omega_h^2 K_e\left(T_m s^2 + s\right)}{D_m K_i\left(s^2 + 2\omega_h \xi s + \omega_h^2\right)} e^{-l} \tag{12}$$

where l -system delay, s.

Since many constant coefficients of the above transfer function are difficult to determine, the identification box of the MATLAB system is used to fit the specific transfer function. Considering that the drive system of the chassis is a large time-delay and nonlinear system, and the maximum time-delay of the system is 150 ms, the transfer function is as follows:

$$\frac{\theta(s)}{u(s)} = \frac{-4.32s^2 + 0.64s}{2250s^2 + 6.4s + 0.0034} e^{-0.15s} \tag{13}$$

Design and Selection of System Hardware

The remote driving system consists of the Web upper computer, the server system and the chassis drive system, as shown in Figure 3. The upper computer is mainly composed of computer equipment that can connect to the internet. The server system consists of the main controller, camera and 4G module. The chassis drive system consists of the lower computer, chassis starting elements, chassis traveling elements, detection elements and PTZ. The starting elements of the chassis include relays, fuel spray nozzle and starter. The chassis traveling elements include the steering engine, double pump and hydraulic motor. The detection elements include speed sensor and inertial measurement unit.

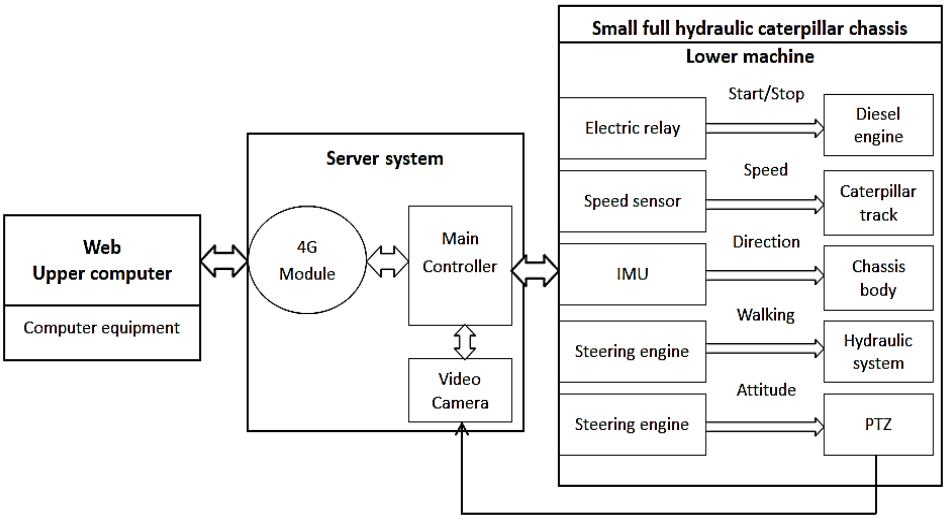

Fig. 3 - Composition and relationship chart of control system

In operation, the main controller sends the image information to the upper computer through the 4G module, and then receives the control command from the upper computer and transmits it to the lower computer. The lower machine controls the start and stop of the diesel engine through ON/OFF of the relay.

The oil pressure of the double-pump and hydraulic motor circuit are controlled by the valve opening of the dual pump controlled by the chassis steering engine, therefore controlling the speed of the hydraulic motor. The traveling speed and direction information of the chassis is obtained by reading the detected data of the encoder and the inertial measurement unit, and the information is uploaded to the upper computer for real-time display. The main controller is mainly used to build the server system, which requires high-speed, multi-transaction processing capabilities and much peripheral interfaces. As shown in Figure 4, the I.MX6U-ALPHA development board is determined to be the main controller. The development board uses I.MX6ULL with Cortex-A7 architecture as the main control chip, the main frequency is 729MHz. The camera provides the video data for the remote control chassis, which requires a certain vision range and good transmission effect. As shown in Figure 5, the HBV-1780-2S2.0 camera is selected. Considering the cost, stability and other factors, EC20 is selected as the 4G network module.

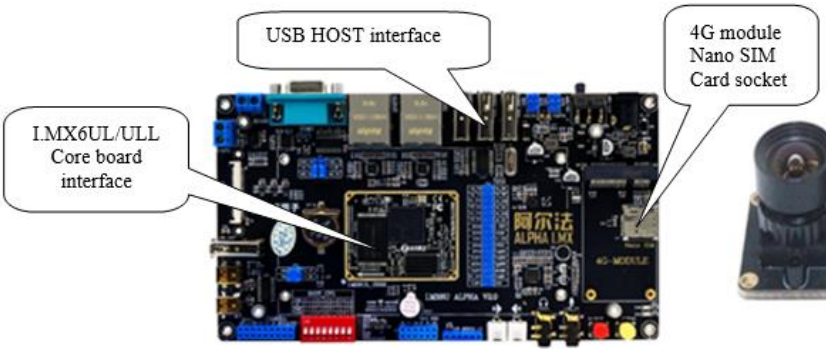

Fig. 4 - I.MX6U-ALPHA development board

Fig. 5 - USB Camera

Considering the requirements of the system for real-time and multitask processing capability, the STM32 core board of ARM architecture is selected as the lower computer. According to the structural characteristics and operating conditions of the chassis, Omron E6B2-CWZ6C is used as the encoder to measure the speed of the chassis. The resolution is 1000P/R, and the input voltage is DC5V-24V. It is installed at the coaxial position of the caterpillar and drive wheel, as shown in Figure 6.

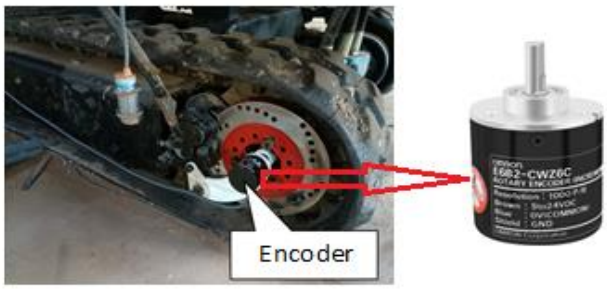

Fig. 6 - Encoder object and installation position

Inertial Measurement Unit (IMU) is used to measure the deflection angle of the chassis. As shown in Figure 7, the six-axis sensor with the chip MPU6050 is selected. It communicates with the main controller through the IIC interface, and the communication rate is 400 kHz. It has an ADC with 16-bit resolution and a DMP digital motion processor. The solution frequency is up to 200 Hz, which can greatly reduce the calculation pressure of the microcontroller.

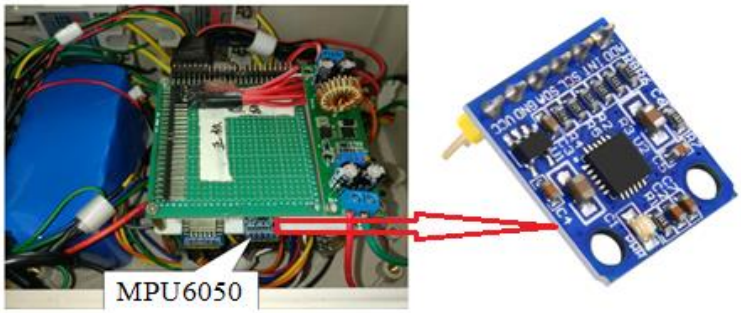

Fig. 7 - Six - axis Sensor and Installation Position

The design and installation of the PTZ should ensure the breadth and depth of the camera's field of view. The PTZ is designed as a 2 DOF mechanism, which can rotate around the x-axis and z-axis by two small steering engines. The top steering engine is used to change the line of sight, and the bottom one is used to change the acquisition range. Therefore, the top steering engine that can rotate 180° is selected, and the bottom steering engine that can rotate 360° is selected. The MG90S is selected as the top steering engine and the SG90 9G is selected as the bottom steering engine. The two steering engine are driven by PWM pulse; the effective high level of the pulse is 0.5 ms-2.5 ms; the response speed of the steering engine is 0.12 sec/60°, and the maximum torque is 1.6 KG/cm. To more comprehensively collect the environmental information, the PTZ is installed in the front of the chassis bridge, as shown in Figure 8.

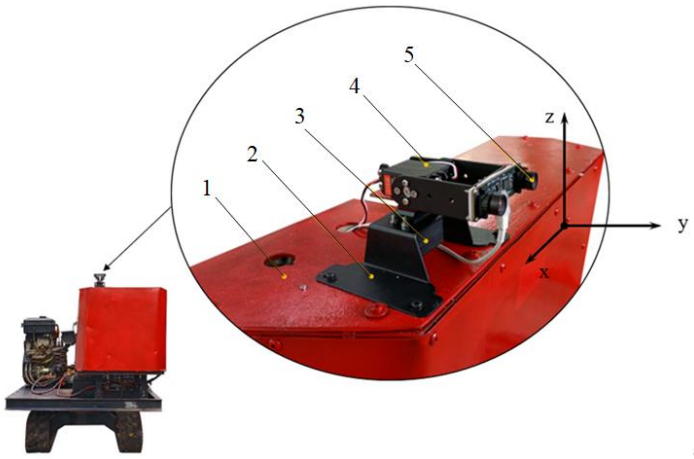

Fig. 8 - Figures of physical objects and installation positions of the pan tilt
1 - Installation platform; 2 – PTZ; 3 - Bottom steering engine; 4 -Top steering engine; 5 -Camera

Design of System Software

The system software is composed of the Web upper computer software, the server system software and the chassis drive system software. The interrelationships and processes are shown in Figure 9.

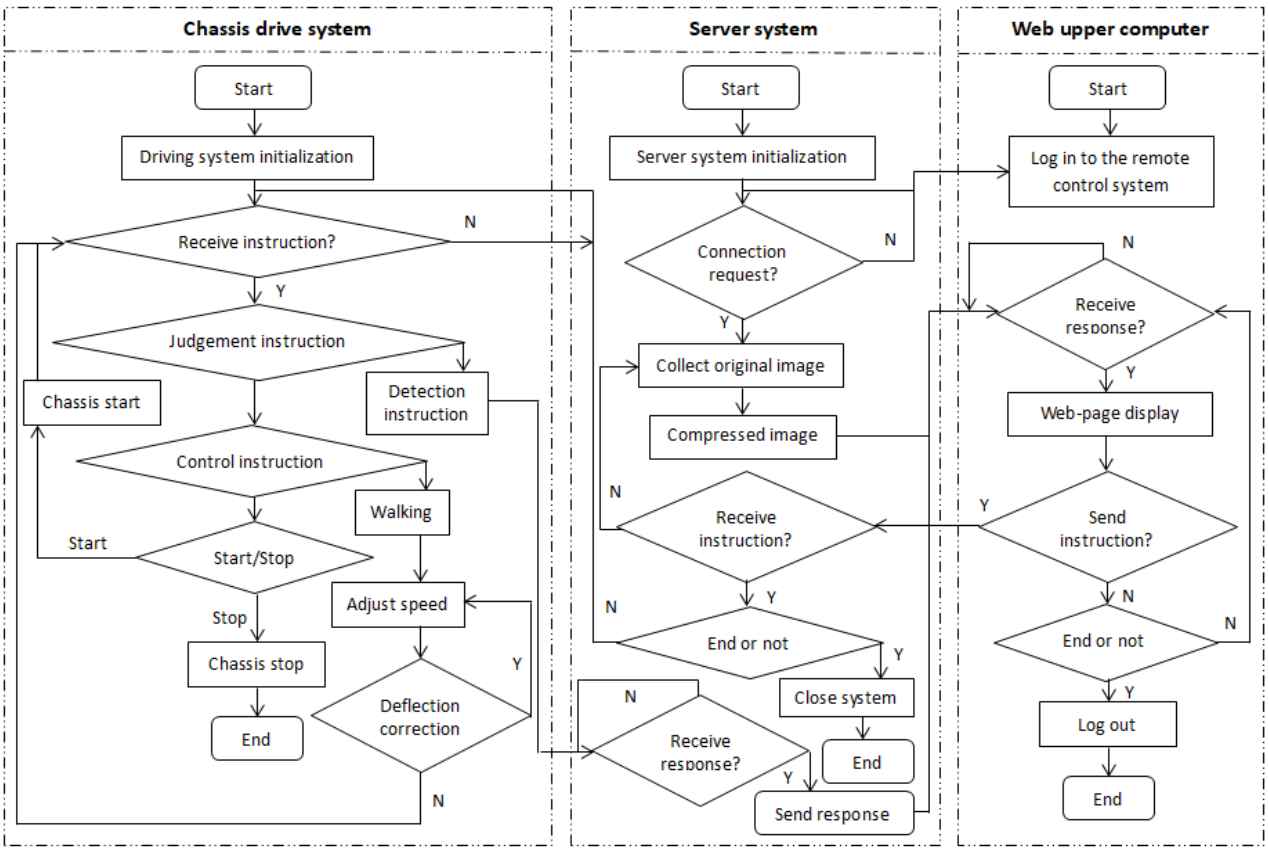

Fig. 9 - Flow chart of software system

The software of the Web upper computer is used to realize the communication function between the remote driving panel and the upper computer. The control commands are sent to the monitoring video through the remote driving panel.

The remote driving Web interface is designed with Bootstrap 3.0 and Ajax technology. The server system software is used to realize the functions of distribution network, video capture, video coding and connection processing. It provides network connection for upper computer and lower computer through Linux operating system.

The network information transmission function of the server system is realized through 4G network. The network channel of the remote control chassis is provided by building a TCP network server. The software of the drive system is used to realize the functions of lower computer communication, chassis drive and detection. With STM32F407 as the control core and MDK5 as the software development platform, the walking control and status detection of the chassis are realized. The lower computer communication is responsible for the data interaction between the upper computer and the lower computer. The timer is used to drive the steering engine to control the movement of the chassis and PTZ. The detection function is used to realize real-time detection of the chassis posture and network status. In this study, the chassis speed is controlled in 0-8 km/h, and the timer is used to measure respectively the output pulses numerical value of (M_{left}, M_{right}) of the left and right encoders. The numerical value of output high-frequency clock pulses is M_{high}, and the output frequency f_{high} is 20 Hz. The basic timer is used to output the sampling pulse, and the data is read once every 50 ms. The M/T method is used to calculate the measured chassis speed v (m/s) by the encoder *(Akkaya et al., 2020; Jia et al., 2018)*.

The calculation is as follows:

$$v = \frac{v_{right} + v_{lift}}{2} = \frac{2\pi r f_{high}}{Z M_{high}} \left(M_{right} + M_{lift} \right) \tag{14}$$

where:

r is the radius of the drive wheel of the chassis, 0.12 m, and z is the solution of the encoder, z=4000P/R.

The six-axis sensor MPU6050 is used as the inertial measurement unit to measure the travel direction angle of the chassis. The lower computer converts the quaternion output by the sensor into Euler angle.

The deflection angle of the chassis is as follows:

$$\emptyset = \tan^{-1}\left(\frac{2wz - 2xy}{w^2 - x^2 + y^2 - z^2}\right) \tag{15}$$

where:

ϕ is the driving deflection angle, and w, x, y, *and* z are the quaternion.

The timer is used to detect the RTT delay between the upper computer and the lower computer. When the time of two adjacent "GET" instructions exceeds the delay threshold, the lower computer reports an exception reminder to ensure the real-time interaction of the system. When the network delay is less than 170 ms, there is little impact on the remote driving. When the network delay is greater than 700 ms, the operability of remote delay will be significantly affected. When the network delay is greater than 1 s, the real-time interactivity of the remote driving can hardly be guaranteed *(Chu et al., 2018; Wang et al., 2018)*. To ensure the smoothness and safety of the remote driving, the delay threshold is set as 1 s.

RESULTS AND ANALYSIS

Steering Performance Test

The real-time interactivity of the remote control system is tested through information transmission during driving and real-time detection of RTT delay. The self-designed hydraulic chassis with a remote driving control system is selected, where the 4G wireless network is used to access the Internet, and the designed software platform is used for remote driving. In the test, the chassis was driven along the specified route at 0.6 m/s. The total travel was about 900 m. The image dates of the surrounding environment and the movement status of the chassis were observed in real time, and the network delay was recorded. The driving route is shown in Figure 10.

Fig. 10 - Roadmap of remote driving

During the chassis driving, the remote control terminal sends the control commands to rotate the PTZ on the chassis, and the surrounding environment images is real-time collected in the front, left, right and rear of the chassis. The real-time test results are shown in Figure 11.

(a) Front environment image (b) Left environment image

(c) Right environment image (d) Rear environment image

Fig. 11 - Image acquisition of the surrounding environment of the chassis

The whole remote driving process takes 28 minutes. During the chassis driving, the RTT delay data is recorded by the upper computer, and the delay data is graphed by MATLAB software. The results are shown in Figure 12.

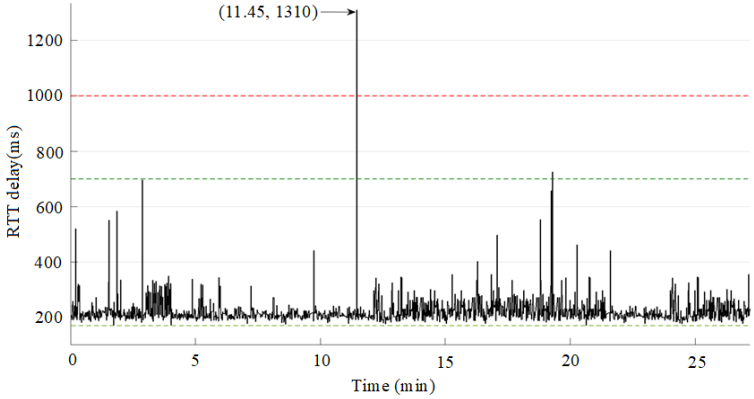

Fig. 12 - RTT delay graph from the upper computer to the lower computer

The test results show that the remote control system can achieve real-time data transmission by the 4G network. The collection for real-time information is flexible; the collected images are complete and accurate, and the image display is stable and smooth, meeting the requirements of the control system for the image collection and transmission of the surrounding environment of the chassis. The remote control system can timely and accurately collect the parameter information in the traveling process of the chassis, and real-time control the chassis for traveling through the instructions. Therefore, the control process is safe and reliable. The delay performance of the control system in Figure 12 shows that the maximum delay time is 1310 ms, which occurs in 11.45 min. At this time, the chassis waits for the network delay to recover within 1000 ms. The minimum delay is 170 ms, occurring at 1.76 min. The delay time occurs twice between 700 m/s and 1000 ms. In this state, the network delay has a significant impact on remote driving. Through calculation, the average RTT delay is 222.75 ms.

CONCLUSIONS

(1) To improve the controllability and safety of the chassis in hilly and mountainous areas, the remote driving control system is designed. The control system can better realize the real-time collection and transmission of the environment images and motion parameters of the chassis through the 4G network. The remote driving control system can realize the remote control of the chassis through human-computer interaction, which is flexible, safe and reliable.

(2) The real-time interaction of the remote driving control system is tested. The test results show that the average delay of data transmission from the upper computer to the lower computer is 222.75 m/s, meeting the requirements of remote driving for real-time interactivity.

(3) The designed control chassis has a certain mechanical delay. Based on the test, the maximum mechanical delay of the chassis is about 100 ms, and the response time of the human brain to sudden situations is about 200 m/s. It can be seen that in case of an emergency, the average delay from the sending of instructions from the upper computer to the execution completion is about 522 ms. When the speed of remote driving chassis is 0.6 m/s, the reaction distance is 0.31 m, meeting the setting requirements of remote control machines.

ACKNOWLEDGEMENT

The study was supported by the National Key Research and Development Program, Key Technologies of Industrialized Agriculture and Intelligent Agricultural Machinery Equipment (2023YFD200050502) and Sichuan Innovation Team of Chinese National Modern Agricultural Industry Technology System (SCCXTD-2024-20).

REFERENCES

[1] Akkaya, R., & Kazan, F. A. (2020). A new method for angular speed measurement with absolute encoder. *Elektronika ir Elektrotechnika*, 26(1), 18-22. https://doi.org/10.5755/j01.eie.26.1.25307

[2] Aliff, M., Raihan, N., Yusof, I., & Samsiah, N. (2019). Development of Remote Operated Vehicle (ROV) Control System using Twincat at Main Control Pod (MCP). *International Journal of Innovative Technology and Exploring Engineering (IJITEE)*, 8(12), 5606-5610. https://doi.org/10.35940/ijitee.L4019.1081219

[3] Alinaghi Hosseinabadi, P., Soltani Sharif Abadi, A., Mekhilef, S., & Pota, H. R. (2020). Chattering-Free Trajectory Tracking Robust Predefined-Time Sliding Mode Control for a Remotely Operated Vehicle. *Journal of Control, Automation and Electrical Systems*, 31, 1177-1195. https://doi.org/10.1007/s40313-020-00599-4

[4] Chu, L. Z., Bai, H. R., Li, J., Wang, F. Y., Guo, R. H., & Sun, Y. (2018). Design of Mobile Robot System Based on the Android System (基于安卓系统农业智能移动机器人的系统设计). *Journal of Agricultural Mechanization Research*, 40(10), 239-242+256. China. https://doi.org/10.13427/j.cnki.njyi.2018.10.046

[5] Cuenca, Á., Zhan, W., Salt, J., Alcaina, J., Tang, C., &Tomizuka, M. (2019). A Remote Control Strategy for an Autonomous Vehicle with Slow Sensor Using Kalman Filtering and Dual-Rate Control. *Sensors*, 19(13), 2983. https://doi.org/10.3390/s19132983

[6] Gázquez, J. A., Castellano, N. N., & Manzano-Agugliaro, F. (2016). Intelligent low cost telecontrol system for agricultural vehicles in harmful environments. *Journal of Cleaner Production*, 113, 204-215. https://doi.org/10.1016/j.jclepro.2015.11.015

[7] Geetha, G., Saranya, G., Meenakshi, K., &Safa, M. (2020). Internet Controlled Remote Vehicle with Live Video Relay and Local Memory. *International Journal of Recent Technology and Engineering (IJRTE)*, 8(5), 4912-4917. https://doi.org/10.35940/ijrte.E5775.018520

[8] Han, K., & Lee, H. (2022). Speed Control of Remotely Operated Multi-Wheel Motor-Driven Vehicles for Unpaved Roads and Obstacles. *International Journal of Automotive Technology*, *23(5)*, 1197-1212. https://doi.org/10.1007/s12239-022-0106-y

[9] Heikkilä, M., Suomalainen, J., Saukko, O., Kippola, T., Lähetkangas, K., Koskela, P., &Posti, H. (2021). Unmanned Agricultural Tractors in Private Mobile Networks. *Network*, 2(1), 1-20. https://doi.org/10.3390/network2010001

[10] Jia, X. D., Wan, Q. H., Zhao, C. H., Du, Y. C., & Yu, H. (2018). Status and Prospect of Velocity Measurement Method with Optical Encoder (光电编码器测速方法现状与展望). *Instrument Technique and Sensor*, (3), 102-107. China.

[11] Kim, J. Y. (2019). A Study of Artificial Intelligence Platform for Vehicle Remote Control: AI Speaker-Based Service Case. *The Journal of Korean Institute of Communications and Information Sciences*, 44(12), 2362-2373. https://doi.org/10.7840/kics.2019.44.12.2362

[12] Liu, C. L., Lin, H. Z., Li, Y. M., Gong, L., & Miao, Z. H. (2020). Analysis on Status and Development Trend of Intelligent Control Technology for Agricultural Equipment(农业装备智能控制技术研究现状与发展趋势分析). *Transactions of the Chinese Society for Agricultural Machinery*, 51(1), 1-18. China.

[13] Liu, X. W. (2018). The path choice of agricultural mechanization development in hilly and mountainous areas (丘陵山区农业机械化发展路径选择). *Modern Agricultural Equipment*, (1), 13-17. China.

[14] Roshanianfard, A., Noguchi, N., Okamoto, H., & Ishii, K. (2020). A review of autonomous agricultural vehicles (The experience of Hokkaido University). *Journal of Terramechanics*, 91, 155-183. https://doi.org/10.1016/j.jterra.2020.06.006

[15] Wang, S., Zhang, S., Ma, R., Jin, E., Liu, X., Tian, H., & Yang, R. (2018). Remote control system based on the Internet and machine vision for tracked vehicles. *Journal of Mechanical Science and Technology*, 32(3), 1317-1331. https://doi.org/10.1007/s12206-018-0236-3

[16] Wang, X.W., Yuan, S.Q., & Jia, W.D. (2022). Current situation and development of agricultural mechanization in hilly and mountainous areas(丘陵山区农业机械化现状与发展). *Journal of Drainage and Irrigation Machinery Engineering*, *40(5)*, 535-540. https://doi.org/10.3969/j.issn.1674-8530.21.0351

[17] Wang, Z., Yang, S., Xiang, X., Vasilijević, A., Mišković, N., & Nađ, Đ. (2020). Cloud-based remote control framework for unmanned surface vehicles. *IFAC-PapersOnLine*, 53(2), 14564-14569. https://doi.org/10.1016/j.ifacol.2020.12.1462

[18] Wu, H.Z., Niu, P., Xie, Y.J., Xia, F., & Wang, M. M. (2022). Present Situation and Suggestions of Agricultural Mechanization in Southwest Hilly and Mountainous Areas (西南丘陵山区农业机械化发展现状及建议). *Agriculture and Technology*, 42(13), 68-70. https://doi.org/10.19754/j.nyyjs.20220715016

[19] Yang, T., & Li, X.X. (2021). Research progress of agricultural machinery autopilot system and analysis of industry competition environment(农机自动驾驶系统研究进展与行业竞争环境分析). *Journal of Chinese Agricultural Mechanization*, 42(11), 222-231.

[20] https://doi.org/ 10.13733/j.jcam.issn.2095-5553.2021.11.33

[21] Zhang, Z.G., Wang, J., Zhu, J.G., Hu, L., & Luo, X.W. (2018). Research progress of auto drive system of agricultural machinery in China. (我国农业机械自动驾驶系统研究进展). *Agriculture Engineering Technology, 38(18),* 23-27. https://doi.org/10.16815/j.cnki.11-5436/s.2018.18.004

[22] Zheng, Y.J., Jiang, S.J., Chen, B.T., Lv, H.T., Wan, C., & Kang, F. (2020). Review on Technology and Equipment of Mechanization in Hilly Orchard (丘陵山区果园机械化技术与装备研究进展). *Transactions of the Chinese Society for Agricultural Machinery*, *51(11)*, 2020, 1-20.

[23] Zhou, L., Wang, G., Sun, K., & Li, X. (2019). Trajectory Tracking Study of Track Vehicles Based on Model Predictive Control. *StrojniškiVestnik - Journal of Mechanical Engineering*, 65(6), 329-342. https://doi.org/10.5545/sv-jme.2019.5980